

Production of ^{129m}Xe and ^{131m}Xe via neutron activation of ^{128}Xe and ^{130}Xe at ILL-RHF and NCBJ-MARIA high-flux reactors

M. Chojnacki ^{a,b,1}, K. Kulesz ^{a,b,1}, I. Michelon ^{a,c}, N. Azaryan ^{a,d}, E. Barbero ^a, B. Crepieux ^a, R. Lica ^{a,e}, Ł. Murawski ^f, M. Ziemba ^f, M. Piersa-Siłkowska ^a, K. Vitulova ^{a,g}, A. Korgul ^h, R.B. Jolivet ⁱ, R. Prokopowicz ^f, U. Köster ^j, M. Kowalska ^{a,b,*}

^a CERN, Espl. des Particules 1, Meyrin, CH-1211, Switzerland

^b University of Geneva, Quai Ernest-Ansermet 24, Geneva, 1211, Switzerland

^c University of Padova, Via 8 Febbraio 2, Padova, 35122, Italy

^d Adam Mickiewicz University, ul. Uniwersytetu Poznańskiego 2, Poznań, 61-614, Poland

^e Horia Hulubei National Institute of Physics and Nuclear Engineering (IFIN-HH), Reactorului 30 St., Bucharest-Magurele, 77125, Romania

^f National Center for Nuclear Research (NCBJ), Andrzeja Soltana 7, Otwock-Swierk, 05-400, Poland

^g Palacky University Olomouc, Krizkovskeho 511/8, Olomouc, CZ-799 00, Czech Republic

^h University of Warsaw, Faculty of Physics, Krakowskie Przedmieście 26/28, Warsaw, 02-093, Poland

ⁱ Maastricht Centre for Systems Biology (MaCSBio), Maastricht University, Paul-Henri Spaaklaan 1, Maastricht, 6229 EN, Netherlands

^j Institut Laue-Langevin (ILL), 71 Avenue des Martyrs, Grenoble, 38000, France

ARTICLE INFO

Keywords:

Neutron activation

Xenon radioisotopes production

ABSTRACT

The long-lived xenon isomers ^{129m}Xe and ^{131m}Xe are of interest for the GAMMA-MRI project, which aims at developing a novel imaging modality based on magnetic resonance of polarized unstable tracers. Here, we present the steps leading to and following the production of these two isomers via neutron irradiation of highly-enriched ^{128}Xe and ^{130}Xe gas samples at two high-flux reactors, the High-Flux Reactor (*Réacteur à haut flux*, RHF) at the Institut Laue-Langevin (ILL) and the MARIA reactor at the National Centre for Nuclear Research (NCBJ). We describe the experimental setups and procedures used to prepare the stable xenon samples, to open the irradiated samples, and to transfer xenon isomers into reusable transport vials. The activity of ^{129m}Xe and ^{131m}Xe was measured to be in the range of tens of MBq per sample of 0.8(1) mg, and was proportional to thermal neutron flux density. A small activity of unstable contaminants was also visible in the samples, but their level is not limiting for the GAMMA-MRI project's objectives. In addition, the minimum thermal neutron flux density required to produce ^{129m}Xe and ^{131m}Xe sufficient for the project could be also determined.

1. Introduction

Neutron activation in nuclear reactors is a well-known approach to large-scale production of long-lived isotopes for medical diagnostics and treatment. The best-known examples of such isotopes are ^{99m}Tc for Single Photon Emission Computed Tomography (SPECT) imaging, ^{131}I for thyroid cancer treatment, and ^{177}Lu for treatment of various types of cancer (IAEA, 2003). However, nuclear reactors can be also used for small-scale production of new isotopes for basic research or pre-clinical studies. Here, we present the production of two such isotopes, long-lived ^{129m}Xe ($T_{1/2} = 8.88$ days) and ^{131m}Xe ($T_{1/2} = 11.84$ days) isomers, using neutron activation of enriched ^{128}Xe and ^{130}Xe at two high-flux reactors, with pre- and post-irradiation handling at the ISOLDE facility

at CERN. This study is part of the GAMMA-MRI project (GAMMA-MRI Collaboration, 2023), whose aim is to develop a new imaging technique based on magnetic resonance imaging (MRI) using polarized unstable tracers (GAMMA-MRI Collaboration, 2021).

The only xenon isotope – ^{133}Xe – which is currently using in medical application (SPECT imaging technique) is produced by uranium target fission. After irradiation, the target is dissolved to extract and purify xenon. This process is a part of other medical isotope (i.e. ^{99m}Tc) production recovery technology from irradiated uranium target (IAEA, 2003; Tachimori and Amano, 1974). The gaseous samples are not commonly used for production of xenon isotopes which can be used directly in medical application. The highly enriched ^{124}Xe is used for ^{125}I production for brachytherapy of prostate cancer, uveal melanomas

* Corresponding author.

E-mail address: magdalena.kowalska@cern.ch (M. Kowalska).

¹ Contributed equally.

Table 1

Relative molar concentration (in %) of other gases in enriched $^{128,130}\text{Xe}$ samples used in irradiations (according to supplier: Isoflex, San Francisco, USA, <https://isoflex.com>).

Xenon sample	^{124}Xe	^{126}Xe	^{128}Xe	^{129}Xe	^{130}Xe	^{131}Xe	^{132}Xe	^{134}Xe	^{136}Xe
Xenon natural abundance	0.1	0.1	1.9	26.4	4.1	21.2	26.9	10.4	8.9
Enriched ^{128}Xe	0.001	0.010	99.931	0.052	0.001	0.001	0.002	0.001	0.001
Enriched ^{130}Xe	0.003	0.003	0.003	0.023	99.947	0.012	0.003	0.003	0.003

Table 2

Relative molar concentration (in %) of xenon isotopes in natural (Kondev et al., 2021) and enriched $^{128,130}\text{Xe}$ samples used in irradiations (according to supplier: Isoflex, San Francisco, USA, <https://isoflex.com>).

Xenon sample	$\text{CO}+\text{N}_2$	CO_2	Ar	CH_4	H_2O	O_2	Kr	C_7H_8
Enriched ^{128}Xe	0.004	0.008	< 0.002	< 0.001	< 0.001	0.002	< 0.004	< 0.002
Enriched ^{130}Xe	0.003	0.011	< 0.006	< 0.001	< 0.009	< 0.005	< 0.006	< 0.005

and brain tumors (IAEA, 2003). For this purpose, ^{124}Xe is enclosed at 10 atm pressure in an aluminium capsule that is then irradiated. However, this method cannot provide pure gaseous samples because the main aim is iodine samples production (Joshi et al., 2012). In comparison, this manuscript presents a unique technique which allows pure and efficient production of gaseous isotopes production for medical applications.

2. Experimental setups and procedures

The production of $^{129\text{m}}\text{Xe}$ and $^{131\text{m}}\text{Xe}$ isomers at the High-Flux Reactor (RHF) at the Institute Laue–Langevin (Guyon and Geltenbort, 2012), and at the MARIA reactor at the National Centre for Nuclear Research (Migdal et al., 2021) and their preparation for further use for the GAMMA-MRI project consisted of several steps spread over several weeks. (a) First, the highly enriched stable ^{128}Xe or ^{130}Xe gases were closed and flame-sealed in quartz vials at CERN. (b) The vials with stable xenon were activated with neutrons for 3–13 days at the RHF or MARIA reactor. 2–5 days after the end of irradiation the activated samples were shipped back to CERN, where: (c) the vials were cleaned from external contamination; (d) γ -ray spectroscopy measurement was performed on the vials; (e) the vials were opened and xenon was transferred to a reusable leak-tight transport vial; (f) γ -ray spectroscopy was performed on the transport vial. In this way, 2–5 days after reception, $^{129\text{m}}\text{Xe}$ or $^{131\text{m}}\text{Xe}$ samples were ready for the next steps in the GAMMA-MRI project. To be conservative, we assume 10 days after the end of irradiation (EOI) the availability of $^{129\text{m}}\text{Xe}$ or $^{131\text{m}}\text{Xe}$ samples for the GAMMA-MRI project. This corresponds to 54% loss of $^{129\text{m}}\text{Xe}$ and 44% loss of $^{131\text{m}}\text{Xe}$ via radioactive decays. In the following, we detail the essential steps and experimental setups.

2.1. Preparation of stable xenon samples for activation

In the first step, highly-enriched ^{128}Xe or ^{130}Xe (enrichment by centrifuge method (Anon., 2023b)) was enclosed in quartz vials – Suprasil 300 quartz glass for RHF reactor or CFQ quartz glass for MARIA reactor – that were flame-sealed by a glass blower. Both, the enrichment and the use of quartz aimed at minimizing the activity of isotopes different than $^{129\text{m}}\text{Xe}$ or $^{131\text{m}}\text{Xe}$. The molar content of other xenon isotopes and other gases in the containers with stable xenon was below 0.1%, as shown in Tables 1 and 2.

The xenon samples were prepared for irradiation using a vacuum-tight gas setup (able to reach $1 \cdot 10^{-5}$ mbar pressure on the pump side, equivalent to $1 \cdot 10^{-3}$ mbar on the xenon bottle side) shown in Fig. 1. The system is made of stainless steel tubing and metal seals (Swagelok, OH, USA) to connect different elements, which guarantees low leak rates and small inner volume, and thus leads to small losses of enriched xenon in ‘dead’ volumes or outside the system.

The xenon filling procedure in the referenced system included the following steps: (a) Two quartz vials (labelled 4. in Fig. 1, 120 mm in

length and closed at one end) were attached via Swagelok-type glass-metal teflon seal to needle valves and through these to the filling setup. (b) All valves in the setup (except the gas-bottle valve) were opened and the whole setup was pumped down with a turbomolecular pump for 48 h. At this point, the pressure measured next to valve number (3.) was $1 \cdot 10^{-5}$ mbar, i.e. about $1 \cdot 10^{-3}$ mbar between the xenon cylinder and the recovery loop (measured offline). (c) The system was purged several times with argon gas at 1000 mbar pressure. (d) The valve to the vacuum pumps (3.) was closed, and (e) the valve at the gas cylinder (1.) was opened to introduce xenon until the gauge 2 (5.) showed 300 mbar (the readout of this gauge was independent of the gas type), and thus the whole setup was filled with ^{128}Xe or ^{130}Xe to that pressure. (f) The needle valves above the quartz vials (4.) were closed to trap inside the vials the quantity of the enriched xenon required for the irradiation. (g) The u-shaped tubing (2.) was placed in a liquid nitrogen bath (LN_2). The remaining xenon was collected in this ‘recovery loop’, since xenon condenses below 165 K. (h) The valve between the recovery loop (2.) and the quartz vials (4.) was closed and the LN_2 trap was removed. (i) The quartz vials with enclosed stable xenon were detached from the setup (j) and sealed with a glass-blowing torch, creating a pair of two 50 mm-long quartz ampoules with about $0.5(1) \text{ cm}^3$ of highly enriched ^{128}Xe or ^{130}Xe at 300 mbar inside (Fig. 2). Finally, xenon trapped in the volume of the u-shape could be used to fill the next two vials, once steps (a) to (i) (except bottle opening at step (e)) were repeated.

After the vials were sealed, the created ampoules were individually cleaned in an ultrasonic bath using consecutively nitric acid, water, and ethyl alcohol. Additionally, ampoules were tested for leaks and fractures by submerging them in water and by heating them in a furnace. The pressure at which xenon was enclosed was chosen to avoid over-pressurization of the ampoules in the reactor core. The maximum pressure inside the vial during the irradiation (300 mbar of enriched xenon in ambient temperature) is lower than 450 mbar inside the RHF reactor (Guyon and Geltenbort, 2012) and 360 mbar inside the MARIA reactor (Marcinkowska and Kulikowska, 2013). The external dimensions of the ampoules, on the other hand, were driven by the size of an enclosure in which the ampoules were placed for the irradiations. Finally, the pressure of stable xenon inside the ampoules of 300(10) mbar and their volume of $0.5(1) \text{ cm}^3$ corresponded to $0.8(1) \text{ mg}$ or $6.1(8) \text{ }\mu\text{mol}$ of xenon inside one ampoule.

2.2. Neutron activation at high-flux reactors

The xenon ampoules were irradiated at two high-flux European reactors, RHF and MARIA, both of which are used for fundamental studies, nuclear physics investigations, as well as production of ‘standard’ and new medical isotopes.

The High-Flux Reactor (RHF) at the Institute Laue–Langevin (ILL) located in Grenoble, France, is one of the most intense sources of thermal neutrons (Guyon and Geltenbort, 2012). To reach thermal conditions ($E_{th} = 25 \text{ meV}$, $v_{th} = 2200 \text{ ms}^{-1}$), the energy spectrum of fission neutrons is moderated by heavy water, D_2O , which is also used

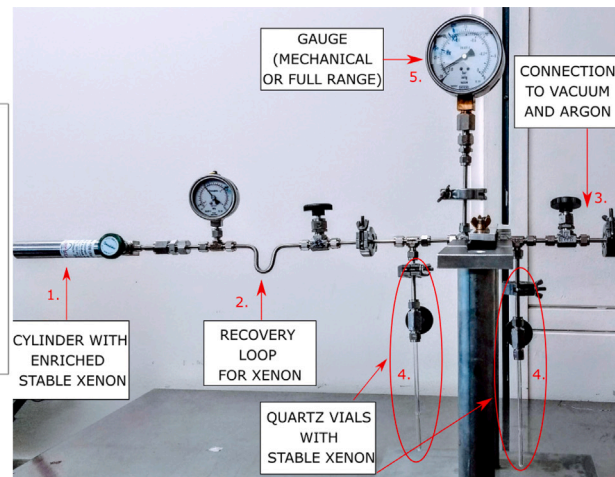
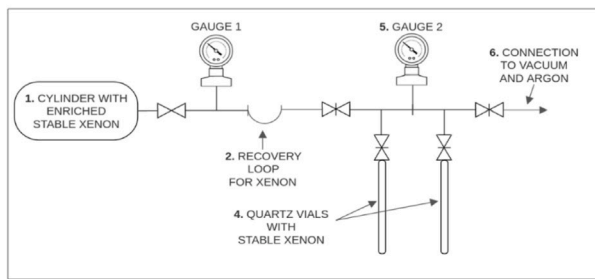


Fig. 1. A schematic drawing (left) and an image (right) of the vacuum-tight gas system used to fill vials with stable xenon. The valves divide the setup into separate volumes.

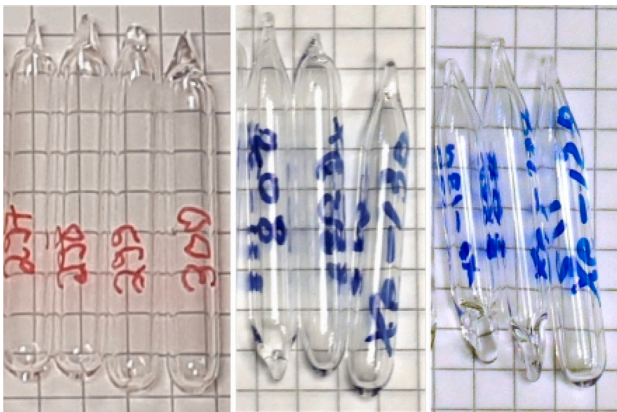


Fig. 2. Several sets of flame-sealed quartz ampoules containing enriched stable xenon. Their outer diameter was 6 mm, inner diameter was 4 mm, while their length was around 50 mm (the spacing between background lines was 5 mm).

as a reactor coolant and neutron reflector (Stacey, 2018). At RHF, the stable xenon samples were irradiated at several positions with the most intense neutron flux density in the reactor, namely $0.7 - 1.1 \cdot 10^{15} \text{ cm}^{-2}\text{s}^{-1}$.

The high-flux reactor MARIA (Migdal et al., 2021) is located at the National Centre for Nuclear Research (NCBJ) in Świerk, Poland. MARIA reactor neutron spectrum is moderated by beryllium blocks and light water, H_2O , that is also used as a reactor coolant (Stacey, 2018). This configuration gives $0.5 - 2.4 \cdot 10^{14} \text{ cm}^{-2}\text{s}^{-1}$ thermal-neutron flux density, which was used to irradiate our xenon samples at several irradiation positions.

The procedures and irradiation times were similar at both reactors. After reception, the stable xenon ampoules were closed inside aluminium capsule, and placed at the irradiation position, where they were irradiated. At the end of the irradiation cycle the capsules were retrieved from the irradiation point and opened. The $^{129\text{m}}\text{Xe}$ or $^{131\text{m}}\text{Xe}$ ampoules were removed from the capsules and shipped to CERN-ISOLDE Class A laboratories. A Posisafe KL-30 type "A" package (Lemer Pax Inc., France) was used, which is a tungsten-shielded hermetic container for the secure transport of all radioactive substances, including gases.

Given the relative molar concentration of enriched xenon ($^{128,130}\text{Xe}$, see Table 2) that is above 99.9%, cross section database (Mughabghab, 2018) and based on the neutron spectrum for both reactors (Guyon and Geltenbort, 2012; Migdal et al., 2021), the following nuclear

reactions: $^{128}\text{Xe}(n, \gamma)^{129\text{m}}\text{Xe}$ or $^{130}\text{Xe}(n, \gamma)^{131\text{m}}\text{Xe}$, should dominate the samples activation. Their cross-sections for thermal neutron energy are presented in Table 3. In addition, other reactions occurring with the nuclei present in the vials with stable xenon or with the nuclei produced during the irradiation should be taken into account as a source of radioactive xenon radioactive isotopes: $^{125,127,133,135,137}\text{Xe}$, xenon isomers: $^{125\text{m},127\text{m},133\text{m},135\text{m}}\text{Xe}$, $^{125,126}\text{I}$ and stable contaminants (Xe stable isotopes: $^{124,126,128-132,134,136}\text{Xe}$) in activated samples. These potential reactions with the corresponding cross-sections are listed in Table 3.

2.3. Cleaning and opening of quartz ampoules, and collection of xenon isomers in transport vials

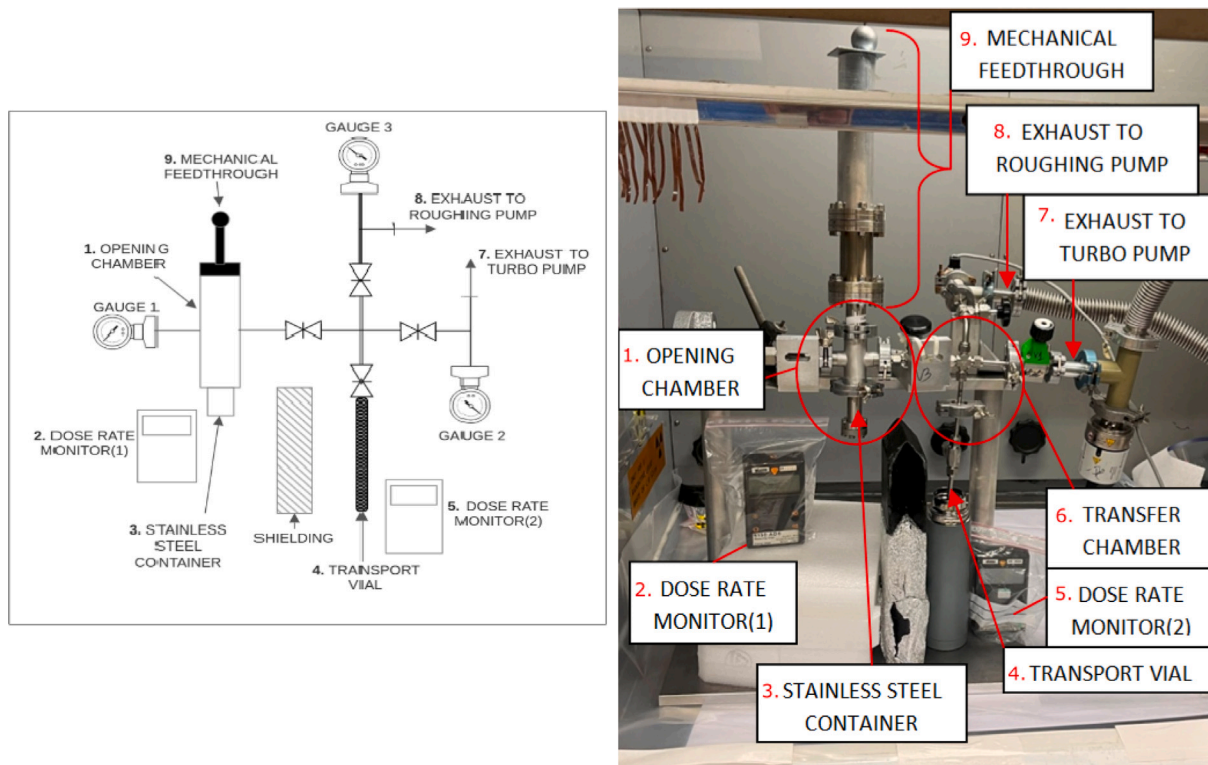
Upon arrival at CERN, activated ampoules were cleaned from contaminants introduced during handling in the reactor hot cells. The cleaning allowed recording of low-background γ -ray spectra of the gases inside the vials, avoiding further contamination, and facilitating radioactive waste management. A standard procedure of decontamination was used: the ampoules were rinsed four times in an ultrasonic bath using sequentially the following solvents: nitric acid 67% solution, demineralized water, ethanol 99% solution, and again demineralized water.

Next, γ -ray spectra were recorded with a calibrated High-Purity Germanium (HPGe) P-type extended range detector (model GX6020 by CANBERRA, Montigny-Le-Bretonneux, France), with a thin carbon window (Anon., 2023a) for each cleaned ampoule in order to establish the produced activity of $^{129\text{m}}\text{Xe}$ or $^{131\text{m}}\text{Xe}$, as well as of other possible unstable contaminants. Finally, the gases inside every quartz ampoule were transferred into a reusable stainless-steel transport vial. For this purpose, the ampoules were crushed and the released xenon isotopes were collected in the transport vial immersed in a LN_2 bath. Other produced isotopes, such as iodine and cesium are solid at room temperature and thus remained in the opening setup.

To avoid contaminating the samples with gaseous air components (N_2 , O_2 , etc.) the opening was carried out using a dedicated vacuum setup (Fig. 3) at low pressure ($5 \cdot 10^{-6}$ mbar, measured with gauge G2). After the vacuum valves between the setup and the pumps were closed (8.), the quartz ampoule was crushed by pushing down onto it with the tip of a mechanical feedthrough (9.). The fact that the quartz ampoule got opened was indicated by a drop in the dose rate measured on the dose monitor 1 (2.). This meant that xenon isomers spread inside the opening chamber. Next, a reusable stainless-steel transport vial equipped with a valve (4.) was cooled in a LN_2 trap for 5 min to perform an efficient xenon transfer from (1.) and collection in (4.). The collection was performed until the dose rate shown by the dose rate

Table 3Average cross sections of thermal-neutron reactions on isotopes present or produced in irradiated samples with enriched $^{128,130}\text{Xe}$ (Mughabghab, 2018).

Reaction	$T_{1/2}$	Cross section (b)	Reaction	$T_{1/2}$	Cross section (b)
$^{128}\text{Xe}(n,\gamma)^{129\text{m}}\text{Xe}$	8.88 d	0.48 (10)	$^{128}\text{Xe}(n,\gamma)^{129}\text{Xe}$	stable	3.0 (7)
$^{130}\text{Xe}(n,\gamma)^{131\text{m}}\text{Xe}$	11.84 d	0.45 (10)	$^{130}\text{Xe}(n,\gamma)^{131}\text{Xe}$	stable	3.1 (7)
$^{124}\text{Xe}(n,\gamma)^{125\text{m}}\text{Xe}$	57 s	28 (5)	$^{124}\text{Xe}(n,\gamma)^{125}\text{Xe}$	16.9 h	122 (21)
$^{125}\text{Xe}(n,\gamma)^{126}\text{Xe}$	stable	< 5600	$^{126}\text{Xe}(n,\gamma)^{127\text{m}}\text{Xe}$	69.2 s	0.25 (13)
$^{126}\text{Xe}(n,\gamma)^{127}\text{Xe}$	36.4 d	2.2 (3)	$^{129}\text{Xe}(n,\gamma)^{130}\text{Xe}$	stable	21 (3)
$^{131}\text{Xe}(n,\gamma)^{132}\text{Xe}$	stable	93 (9)	$^{132}\text{Xe}(n,\gamma)^{133\text{m}}\text{Xe}$	2.2 d	0.005 (1)
$^{132}\text{Xe}(n,\gamma)^{133}\text{Xe}$	5.2 d	0.40 (6)	$^{133}\text{Xe}(n,\gamma)^{134}\text{Xe}$	stable	190 (90)
$^{134}\text{Xe}(n,\gamma)^{135\text{m}}\text{Xe}$	9.1 h	0.003 (1)	$^{134}\text{Xe}(n,\gamma)^{135}\text{Xe}$	15.6 min	0.003 (1)
$^{134}\text{Xe}(n,\gamma)^{135}\text{Xe}$	9.14 h	0.26 (3)	$^{135}\text{Xe}(n,\gamma)^{136}\text{Xe}$	stable	2.65 (11)
$^{136}\text{Xe}(n,\gamma)^{137}\text{Xe}$	3.8 min	0.26 (2)			

**Fig. 3.** Schematic drawing (left) and photograph (right) of the setup used for opening quartz ampoules.

monitor 2 (5.) was close to that observed originally at the dose rate monitor 1 (2.) and did not change further. At that point, the needle valve on the transport vial was closed. Next, the rest of the system was pumped and the transport vial was detached from the setup.

After the opening procedure, the filled transport vials were moved to the γ -ray spectroscopy station for activity measurements of the trapped gases. Based on those measurements and the measurements performed earlier on the decontaminated quartz ampoules, a collection efficiency (ϵ_{col}) was established for each sample.

3. Results

3.1. Cross sections for $^{129\text{m}}\text{Xe}$ and $^{131\text{m}}\text{Xe}$ production

The γ -ray spectroscopy measurements performed on decontaminated quartz tubes showed activities above 40 MBq per sample for $^{129\text{m}}\text{Xe}$ and $^{131\text{m}}\text{Xe}$ produced in both reactors. These activities exceeded the requirement of the GAMMA-MRI project for the minimum total activity of 10 MBq measured 10 days after the end of irradiation (EOI) (GAMMA-MRI Collaboration, 2021). Figs. 4 and 5 show the

experimental results from a dozen ampoules irradiated at RHF and MARIA reactors. The measured activities are determined for the end of irradiation and normalized to the number of moles ($\text{MBq} \cdot \mu\text{mol}^{-1}$). The activities uncertainty includes vial volume uncertainty (10%) of the enclosed stable xenon gas, as well as a smaller contribution from the uncertainty of gamma spectroscopy measurement. The neutron flux densities are extracted from calculations made in Monte Carlo N-Particle Transport Code (MCNP) (Calzavara et al., 2011; Marcinkowska and Kulikowska, 2013) with uncertainty based on the fluctuation of the reactor exploitation parameters (about 10%–15%).

Fig. 4 shows experimental data for $^{129\text{m}}\text{Xe}$ (blue dots with error bars). Based on measured activities and linear activation law (IAEA, 1990), the cross-section for radiative neutron capture reaction on ^{128}Xe in a Maxwellian thermal neutron flux was fitted (solid orange line with orange uncertainty area), $\sigma_{\gamma}(^{128}\text{Xe}) = 0.29(1)$ b. Fitted cross-section is 40% lower than the recommended literature value (Mughabghab, 2018). Finally, considering neutron capture on $^{129\text{m}}\text{Xe}$, the simultaneous contributions of neutron captures on ^{128}Xe and $^{129\text{m}}\text{Xe}$ (“destroying” $^{129\text{m}}\text{Xe}$) (Cetnar, 2006) were fitted. This approach gave the

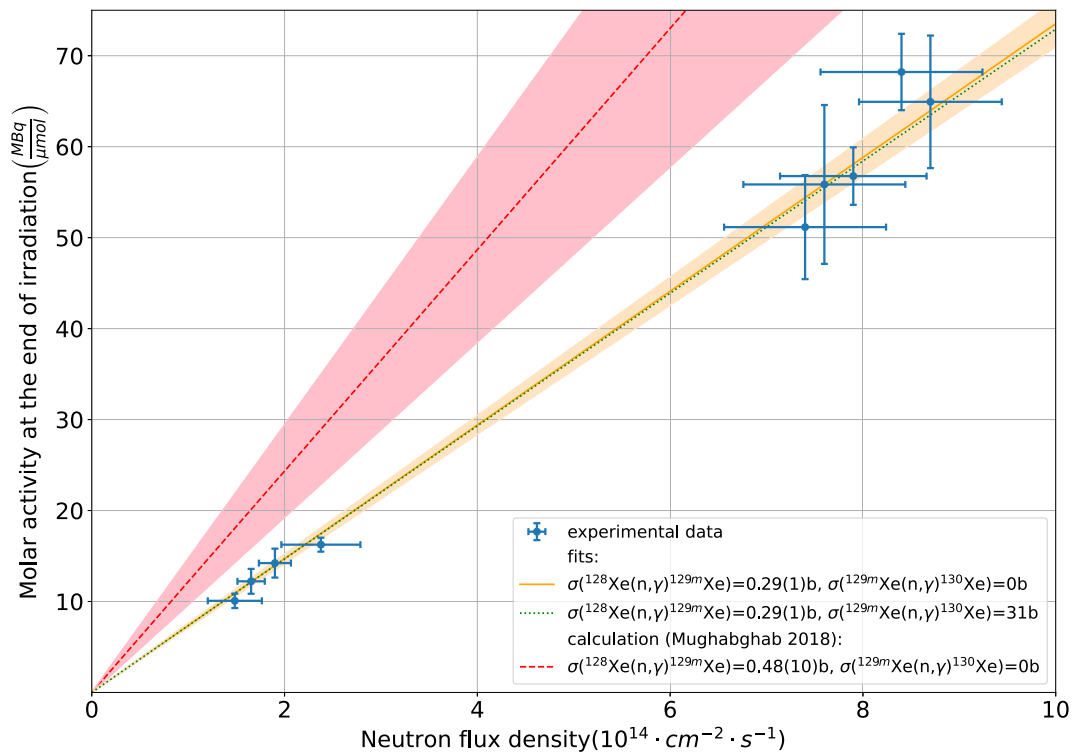


Fig. 4. ^{129m}Xe production rates (molar activities at the end of irradiation) for samples irradiated in different neutron flux densities in the RHF and MARIA reactors (blue points with uncertainties — see text for details about uncertainties). Fitted cross-section for radiative neutron capture reactions on ^{128}Xe (solid orange curve) with uncertainty range (orange area). Fitted upper limits for radiative neutron capture reaction on ^{129m}Xe (dotted green curve). Calculated activities (dashed red curve) with uncertainty range (pink area) based on Mughabghab (2018).

unchanged value for $\sigma_\gamma(^{128}\text{Xe})$ compared to the linear activation law and allowed to set an upper limit, defined as fitted value (close to zero) plus one standard deviation value, for radiative cross-section on ^{129m}Xe , $\sigma_\gamma(^{129m}\text{Xe}) < 31$ b (dotted green line).

Data for ^{131m}Xe , presented in Fig. 5, shows a good agreement between molar activities at the end of irradiation expected from literature cross-section value (dashed red line with pink uncertainty area) (Mughabghab, 2018) and experimental data (blue dots with error bars). Fitted experimental cross-section for radiative neutron capture on ^{130}Xe in Maxwellian thermal flux (solid orange line) is $\sigma_\gamma(^{130}\text{Xe}) = 0.41(2)$ b. Taking into account radiative cross-section on ^{131m}Xe (Cetnar, 2006) gives the similar result for radiative neutron capture on stable ^{130}Xe and allows to estimate the upper limit, defined as fitted value (close to zero) plus one standard deviation value, for radiative cross-section on ^{131m}Xe , $\sigma_\gamma(^{131m}\text{Xe}) < 75$ b (dotted green line).

3.2. Radionuclide purity

The γ -ray spectroscopy measurements allowed also to determine the radionuclide purity of ^{129m}Xe and ^{131m}Xe samples, expressed as a percentage of the radioactivity of the desired radionuclide to the total radioactivity of the source. Radionuclide purity is important for isotopes that are planned to be used in medical applications as the present impurities may increase the effective dose rate received by the patient, thus degrading the quality of any imaging procedure performed (IAEA, 2023). The limits set for ^{129m}Xe and ^{131m}Xe samples are presented in Table 4.

3.3. Xenon collection efficiency

The main parameter that can characterize the setup used to open the irradiated ampoules and to enclose xenon in reusable metallic transport vials (Fig. 3), is the xenon collection efficiency (ϵ_{col}). The parameter ϵ_{col}

was determined based on γ -ray spectroscopy measurements performed on sealed quartz ampoules with activated ^{129m}Xe or ^{131m}Xe and then on corresponding transport vials with transferred xenon. To factor out the loss in activity due to radioactive decay, the measured activities after transfer have been recalculated to the start time of the measurement on the corresponding quartz vial. For that, it is required to have a good estimation of γ -ray efficiency of the relevant γ -ray lines of ^{129m}Xe and ^{131m}Xe for both geometries (i.e. quartz ampoules and metal container). Our estimates are based on the Nucleonica package, followed by a more precise determination using Geant4 simulations. The value of ϵ_{col} is relevant for the GAMMA-MRI project since its high value allows to maintain a high level of ^{129m}Xe or ^{131m}Xe activity received from the reactors to make it available for further use within the project. Based on a dozen collections, the average value of ϵ_{col} was around 75(4)%.

3.4. Minimum thermal neutron flux density requirements

Based on GAMMA-MRI project requirements (mentioned in Section 3.1) the minimum xenon isomers activity required for the project is 10 MBq (A_{min}) 10 days after the end of irradiation (t_d). Following this requirement and neutron activation principles, the minimum required thermal neutron flux density (ϕ_{th}) for continuous irradiation is described by the equation (IAEA, 1990):

$$\phi_{th} \geq \frac{A_{min}}{\epsilon_{col} \cdot \sigma_{\gamma,i} \cdot n \cdot N_A \cdot (1 - \exp(-\lambda_j \cdot t_{irr})) \cdot \exp(-\lambda_j \cdot t_d)},$$

where $\sigma_{\gamma,i}$ — cross section for radiative neutron capture reaction on isotope i (^{128}Xe or ^{130}Xe) obtained from experimental data (Section 3.1), n — number of moles of isotope i presents in irradiated sample, N_A — Avogadro number, t_{irr} — irradiation time, λ_j — decay constant of produced isomer j (^{129m}Xe or ^{131m}Xe), ϵ_{col} — xenon collection efficiency (Section 3.3). The graphical representation of minimum thermal neutron flux density required for GAMMA-MRI project, calculated for 6.1 μmol (average irradiated quantity of stable xenon - Section 2.1), is presented in Fig. 6.

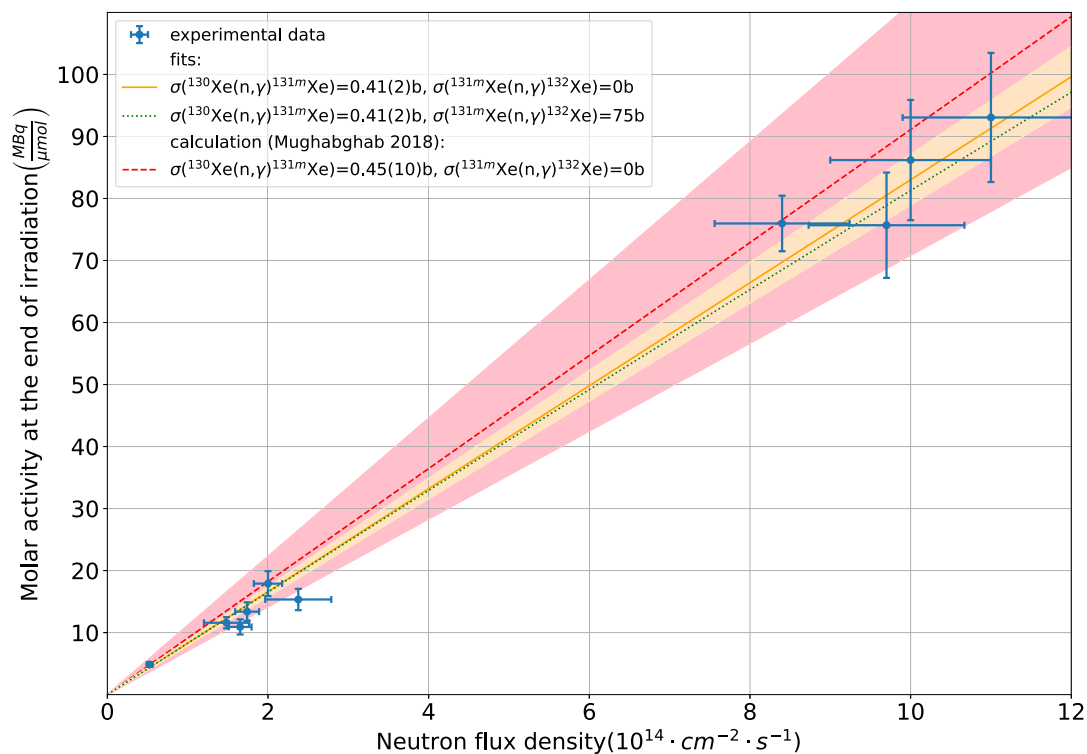


Fig. 5. ^{131m}Xe production rates (molar activities at the end of irradiation) for samples irradiated in different neutron flux densities in the RHF and MARIA reactors (blue points with uncertainties — see text for details about uncertainties). Fitted cross-section for radiative neutron capture reactions on ¹³⁰Xe (solid orange curve) with uncertainty range (orange area). Fitted upper limits for radiative neutron capture reaction on ^{131m}Xe (dotted green curve). Calculated activities (dashed red curve) with uncertainty range (pink area) based on Mughabghab (2018).

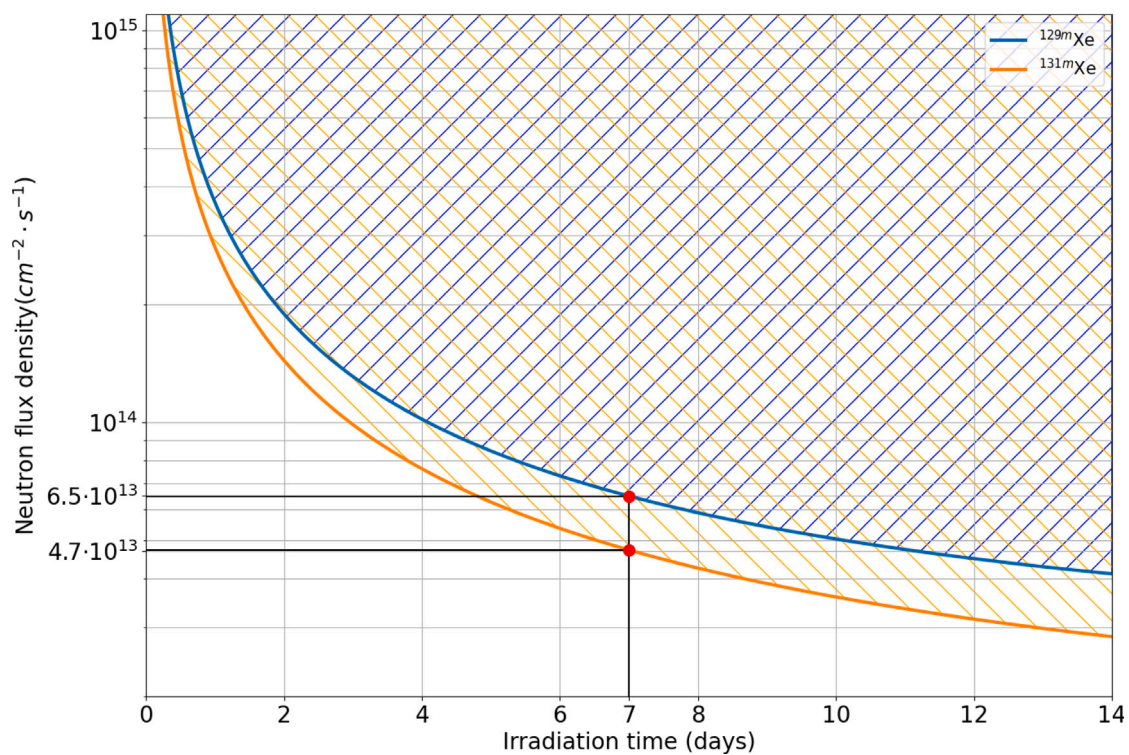


Fig. 6. Minimum thermal neutron flux density in function of continuous irradiation time necessary to reach the GAMMA-MRI objective of 10 MBq of xenon isomer in the transport container 10 days after end of irradiation: flux requirement for ^{129m}Xe (blue dashed area) and ^{131m}Xe (orange dashed area). As an example flux requirement for 7 days irradiation for ^{129m}Xe (red point on the blue curve) and ^{131m}Xe (red point on the orange curve).

Table 4

Radionuclide purity of ^{129m}Xe and ^{131m}Xe samples, produced in high-flux nuclear reactors, 5 days and 10 days after the end of irradiation (EOI). Isotopes other than xenon (e.g I and Cs) remained in the glass ampoules so were not visible in transport vials. All values have been determined from gamma spectroscopy measurements. These without an asterisk are based on fitting a visible gamma peak. For those with an asterisk, no gamma peak was visible at the expected energy, and thus their upper limits were based on the estimation of the Minimum Detectable Activity (MDA) (Debertin and Helmer, 2001).

Date	Sample	^{129m}Xe	^{131m}Xe	^{125}Xe	^{127}Xe	^{133}Xe	^{133m}Xe	^{135}Xe
EOI+5 days	^{129m}Xe	> 99.72%	< 0.21%*	< 0.005%	< 0.03%	< 0.01%*	< 0.02%*	< 6E-04%*
EOI+10 days	^{129m}Xe	> 99.72%	< 0.23%*	< 5E-05%	< 0.04%	< 0.008%*	< 0.006%*	< 1E-07%*
EOI+5 days	^{131m}Xe	< 0.05%*	> 99.91%	< 0.005%*	< 0.004%*	< 0.007%*	< 0.02%*	< 0.005%*
EOI+10 days	^{131m}Xe	< 0.05%*	> 99.94%	< 5E-05%*	< 0.004%*	< 0.005%*	< 0.006%*	< 7E-08%*

4. Conclusions and outlook

In the above manuscript, we have described the experimental setups and procedures (Section 2.1) which allowed to obtain samples of ^{129m}Xe and ^{131m}Xe for the GAMMA-MRI project via irradiation of enriched ^{128}Xe and ^{130}Xe at high-flux reactors (Sections 2.2 and 2.3). The setups use commercial vacuum elements and Swagelok-type tube connectors, which allow achieving 10^{-5} mbar pressure on the side of the vacuum pumps and 10^{-3} mbar on the other extreme (see Figs. 1 and 3). Liquid nitrogen traps were used to collect stable and unstable xenon gases in the desired volumes.

We have also shown the production rates, i.e. activities normalized to the number of moles of stable xenon inside samples at the end of irradiation, for ^{129m}Xe and ^{131m}Xe . These results allowed to calculate cross-section for radiative neutron capture on ^{128}Xe (0.29(1) b) and ^{130}Xe (0.41(2) b). Additionally, upper limits for cross sections for radiative neutron capture on ^{129m}Xe (< 31 b) and ^{131m}Xe (< 75 b) were established (Section 3.1).

The radionuclide purity of ^{129m}Xe and ^{131m}Xe produced in nuclear reactor have been defined (Section 3.2, Table 4). Furthermore, the minimum thermal neutron density required to produce intense ^{129m}Xe and ^{131m}Xe samples for the future of GAMMA-MRI project have been established (Section 3.4, Fig. 6).

An efficient production method of ^{129m}Xe and ^{131m}Xe in high-flux neutron reactors was established for the GAMMA-MRI project. This approach already provides high-activity and relatively high-purity samples. To characterize the samples in more detail and to maximize the available activity, the next steps in the project are analysis of sample composition before irradiation, longer γ -ray measurement for irradiated ampoules, upgrading the experimental setups allowing to reach better vacuum and higher efficiency of xenon transfer. Also, thermal neutron cross-section studies should be performed to better understand the sources of unstable contaminants and the ways to minimize them. These studies can allow the prediction of the composition of $^{129m,131m}\text{Xe}$ samples at different reactor facilities and, subsequently, the irradiation optimization.

CRediT authorship contribution statement

M. Chojnacki: Writing – review & editing, Writing – original draft, Visualization, Methodology, Investigation, Formal analysis, Data curation, Conceptualization. **K. Kulesz:** Writing – review & editing, Writing – original draft, Methodology, Investigation, Conceptualization. **I. Michelon:** Methodology, Investigation. **N. Azaryan:** Conceptualization. **E. Barbero:** Conceptualization. **B. Crepieux:** Conceptualization. **R. Lica:** Software, Resources, Methodology, Investigation. **Ł. Murawski:** Resources, Investigation, Conceptualization. **M. Ziemia:** Software, Resources, Investigation, Conceptualization. **M. Piersa-Siłkowska:** Investigation. **K. Vitulova:** Investigation. **A. Korgul:** Resources, Methodology, Investigation. **R.B. Jolivet:** Supervision, Resources, Project administration, Conceptualization. **R. Prokopowicz:** Resources, Investigation, Conceptualization. **U. Köster:** Validation, Resources, Methodology, Investigation, Conceptualization. **M. Kowalska:** Validation, Supervision, Resources, Project administration, Methodology, Investigation, Conceptualization.

Declaration of competing interest

The authors declare the following financial interests/personal relationships which may be considered as potential competing interests: Karolina Kulesz reports financial support was provided by Swiss Excellence Government Scholarship. Magdalena Kowalska reports financial support was provided by CERN Medical Application Fund. Renaud B.Jolivet reports financial support was provided by CERN Medical Application Fund. Gamma-MRI collaboration reports financial support was provided by European Union Horizon 2020. Agnieszka Korgul reports financial support was provided by Polish Ministry of Education and Science. Rafal Prokopowicz reports financial support was provided by Polish Ministry of Education and Science. Lukasz Murawski reports financial support was provided by Polish Ministry of Education and Science. Maciej Ziemia reports financial support was provided by Polish Ministry of Education and Science. Razvan Lica reports financial support was provided by Romanian IFA grant. Razvan Lica reports financial support was provided by Nucleu project No. PN 23 21 01 02.

Data availability

Data will be made available on request.

Acknowledgements

This project received funding from the Swiss Excellence Government Scholarship (to KK), the CERN Medical Application Fund (gamma-MRI; to RBJ and MK), the European Union's Horizon 2020 research and innovation programme under grant agreement No 964644 (GAMMA-MRI). AK and RP, ŁM, MZ acknowledge funding from the Polish Ministry of Education and Science. RL acknowledges the Romanian IFA grant CERN/ISOLDE and Nucleu project No. PN 23 21 01 02.

References

- Anon., 2023a. Extended range coaxial ge detectors. <https://www.gammadata.se/assets/Uploads/XtRa-detectors-C49310.pdf>. (Accessed 20 May 2023).
- Anon., 2023b. Isoflex company website with enrichment methods information. <https://www.isoflex.com/products/periodic-table>. (Accessed 12 December 2023).
- Calzavara, Y., Fuard, S., Bergeron, A., 2011. Evaluation of measurements performed on the French high flux reactor (RHF). Benchmark RHF-FUND-RESR-001.
- Cetnar, J., 2006. General solution of bateman equations for nuclear transmutations. *Ann. Nucl. Energy* 33, 640–645. <http://dx.doi.org/10.1016/j.anucene.2006.02.004>.
- Debertin, K., Helmer, R., 2001. *Gamma and X-Ray Spectrometry with Semiconductor Detectors*. Elsevier Science.
- GAMMA-MRI Collaboration, 2021. *Gamma-MRI: The future of molecular imaging*. Grant agreement ID: 964644.
- GAMMA-MRI Collaboration, 2023. GAMMA-MRI collaboration website. <https://gamma-mri.eu>. (Accessed 26 July 2023).
- Guyon, H., Geltenbort, P., 2012. The high flux research reactor at the Laue-Langevin institute (ILL). *Atw Int. Z. Kernenerg.* 57 (10).
- IAEA, 1990. *Practical Aspects of Operating a Neutron Activation Analysis Laboratory*. TECDOC Series, (564), International Atomic Energy Agency, Vienna, URL https://www-pub.iaea.org/MTCD/publications/PDF/te_564_web.pdf.
- IAEA, 2003. *Manual for Reactor Produced Radioisotopes*. TECDOC Series, (1340), International Atomic Energy Agency, Vienna, URL <https://www.iaea.org/publications/6407/manual-for-reactor-produced-radioisotopes>.

- IAEA, 2023. Human health campus website. <https://humanhealth.iaea.org/HHW/>. (Accessed 1 August 2023).
- Joshi, P.V., et al., 2012. Production of iodine-125 from neutron irradiation of natural Xe gas and aWet distillation process for radiopharmaceutical applications. *Ind. Eng. Chem. Res.* 51 (25), 8575–8582.
- Kondev, F.G., Wang, M., Huang, W.J., Naimi, S., Audi, G., 2021. The NUBASE2020 evaluation of nuclear properties. *Chin. Phys. C* 45 (3), <http://dx.doi.org/10.1088/1674-1137/abddae>.
- Marcinkowska, Z.E., Kulikowska, T.A., 2013. Reliability of neutronics characteristics prediction for reactor maria core conversion to LEU fuel. *Ann. Nucl. Energy* 59, 92–99. <http://dx.doi.org/10.1016/j.anucene.2013.03.042>, URL <https://www.sciencedirect.com/science/article/pii/S0306454913001801>.
- Migdal, M., et al., 2021. MARIA reactor irradiation technology capabilities towards advanced applications. *Energies* 14 (23), <http://dx.doi.org/10.3390/en14238153>.
- Mughabghab, S., 2018. Atlas of Neutron Resonances, sixth ed. In: Resonance Properties and Thermal Cross Sections Z = 1–60, vol. 1, National Nuclear Data Center, Brokhaven National Laboratory, <http://dx.doi.org/10.1016/C2015-0-00522-6>.
- Stacey, W., 2018. *Nuclear Reactor Physics*, 3rd Edition. John Wiley & Sons.
- Tachimori, S., Amano, H., 1974. Preliminary study on production of Xenon-133 from neutron-irradiated uranium metal and oxides by pxdation. *J. Nucl. Sci. Technol.* 11 (11), 488–494.